Supplementary Information for "Important role of stratosphere-troposphere coupling in the Arctic mid-to-upper tropospheric warming in response to sea-ice loss"

Mian Xu[1], Wenshou Tian[1]*, Jiankai Zhang[1]*, James A. Screen[2], Chongyang Zhang[1], Zhe Wang[1]

1. College of Atmospheric Sciences, Lanzhou University, China

2. Department of Mathematics and Statistics, University of Exeter, Exeter, UK

*** Corresponding authors: Wenshou Tian, wstian@lzu.edu.cn; Jiankai Zhang, jkzhang@lzu.edu.cn**

Supplementary Figures

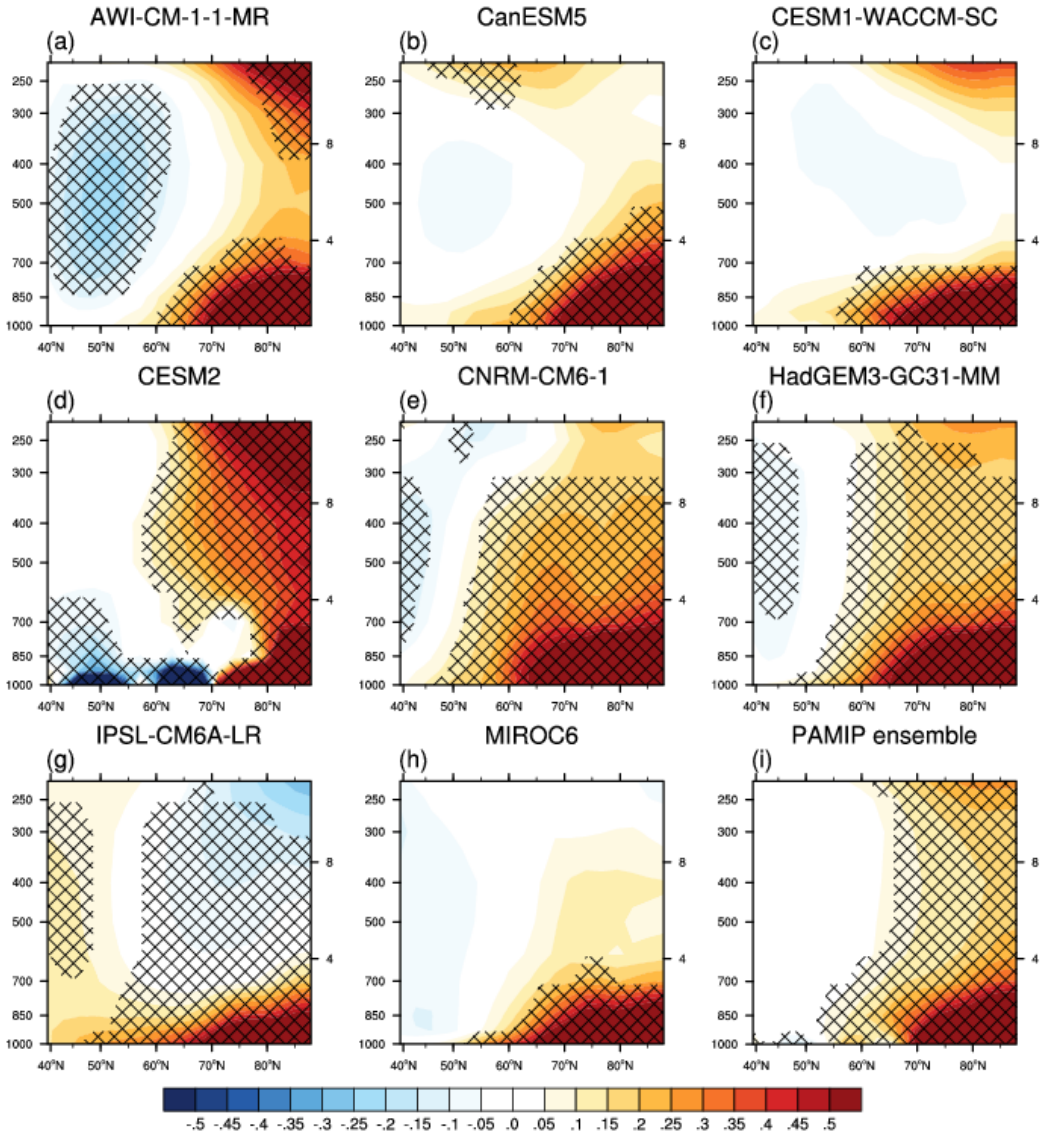

Supplementary Figure 1. Zonal-mean winter temperature anomalies induced by BKS sea-ice loss simulated by PAMIP models. Simulated wintertime zonal-mean temperature differences (K) between pdSST-futBKSeasSIC and pdSST-pdSIC runs from (a) AWI-CM-1-1-MR, (b) CanESM5, (c) CESM1-WACCM-SC, (d) CESM2, (e) CNRM-CM6-1, (f) HadGEM3-GC31-MM, (g) IPSL-CM6A-LR, (h) MIROC6 and (i) PAMIP multi-model ensemble mean. All the results are scaled by the ratio of the

observed BKS SIC differences between low- and high-SIC years and PAMIP SIC forcing. Hatched regions are statistically significant at the 90% confidence level according to bootstrap resampling statistical test.

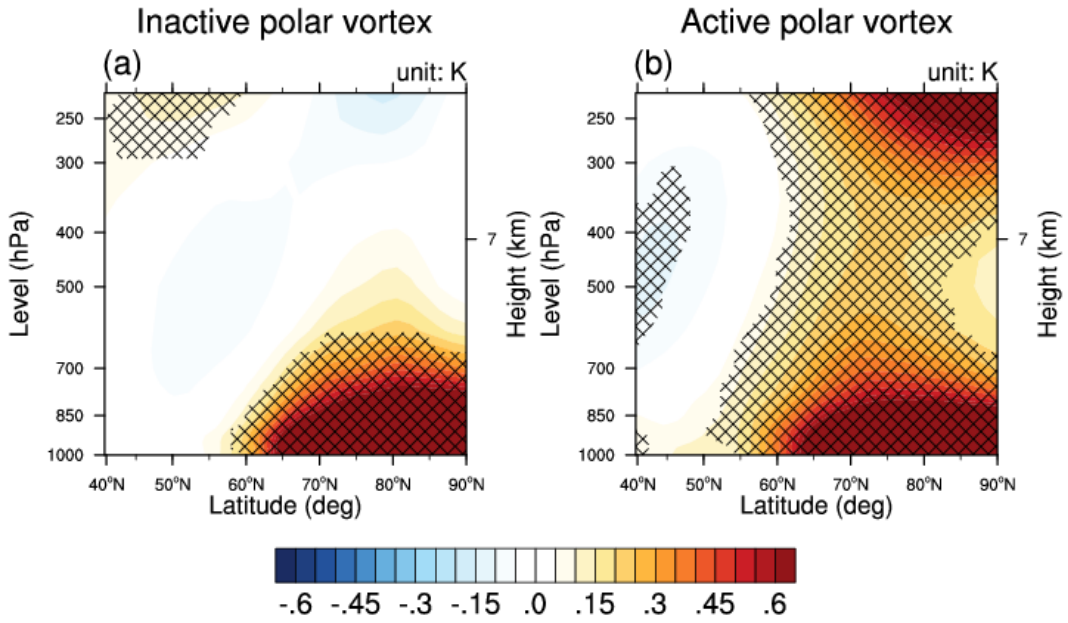

Supplementary Figure 2. Zonal-mean winter temperature anomalies induced by BKS sea-ice loss in inactive- and active-polar-vortex years. (a) Simulated zonal-mean winter temperature differences (K) between LICE and HICE runs averaged in inactive-polar-vortex years, derived from free-running WACCM-SC simulations. (b) the same as (a), but for the temperature differences between the active-polar-vortex years in LICE and HICE run. Hatched regions are statistically significant at the 90% confidence level according to bootstrap resampling statistical test.

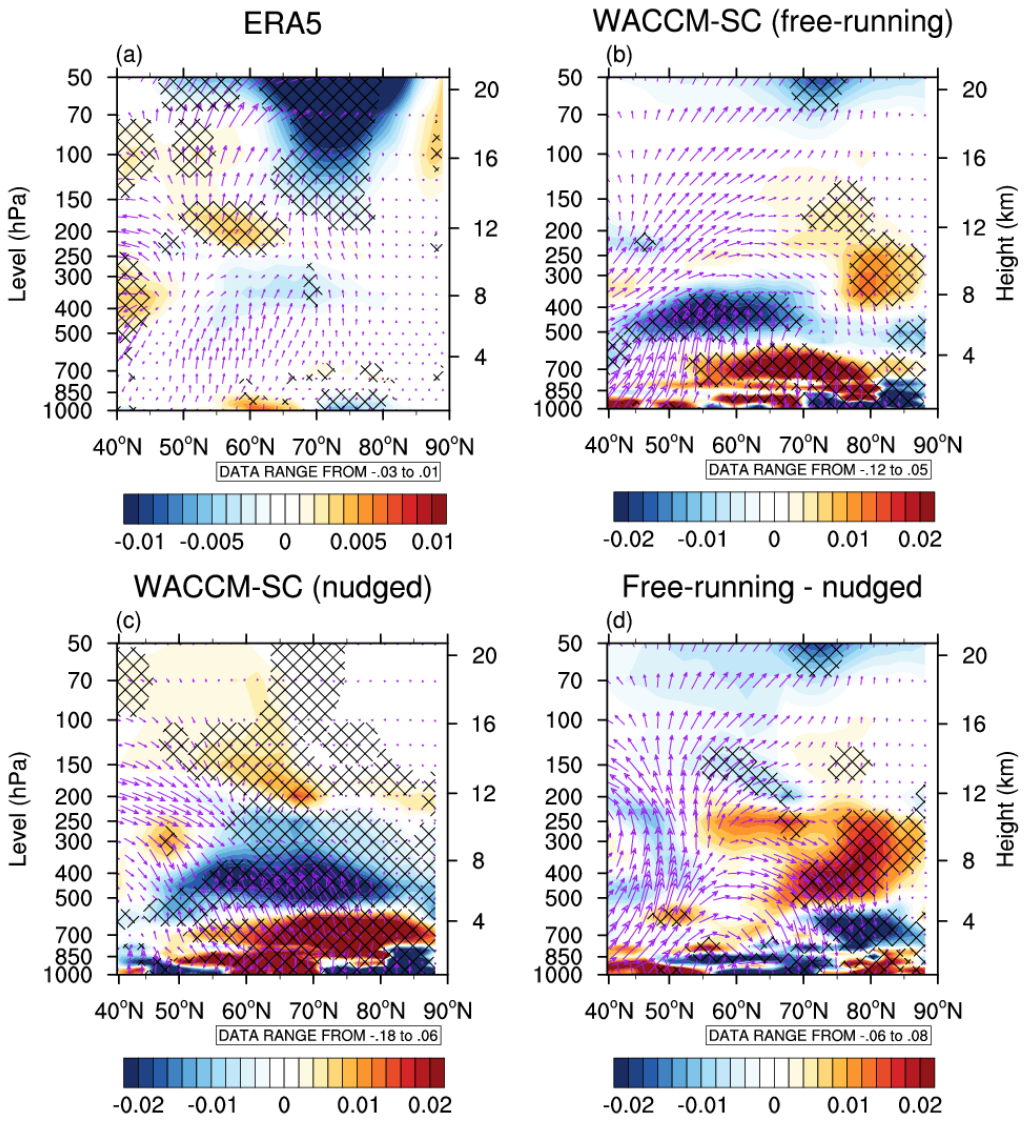

Supplementary Figure 3. Winter E-P flux anomalies induced by BKS sea-ice loss. (a) EP fluxes (purple arrows; scaled by air pressure; the vertical component is scaled by 10^4 and the meridional component is scaled by 10^6; m s^{-2}) and their divergence (shading; s^{-2}) regressed against BKS sea ice from ERA5 reanalysis, scaled by the composited SIC differences between BKS low- and high-SIC years. Simulated differences of EP flux and its divergence between LICE and HICE runs in the (b) free-running WACCM-SC simulations, (c) nudged WACCM-SC simulations, and (d) their differences. Hatched regions are statistically significant at the 90% confidence level according to bootstrap resampling statistical test.

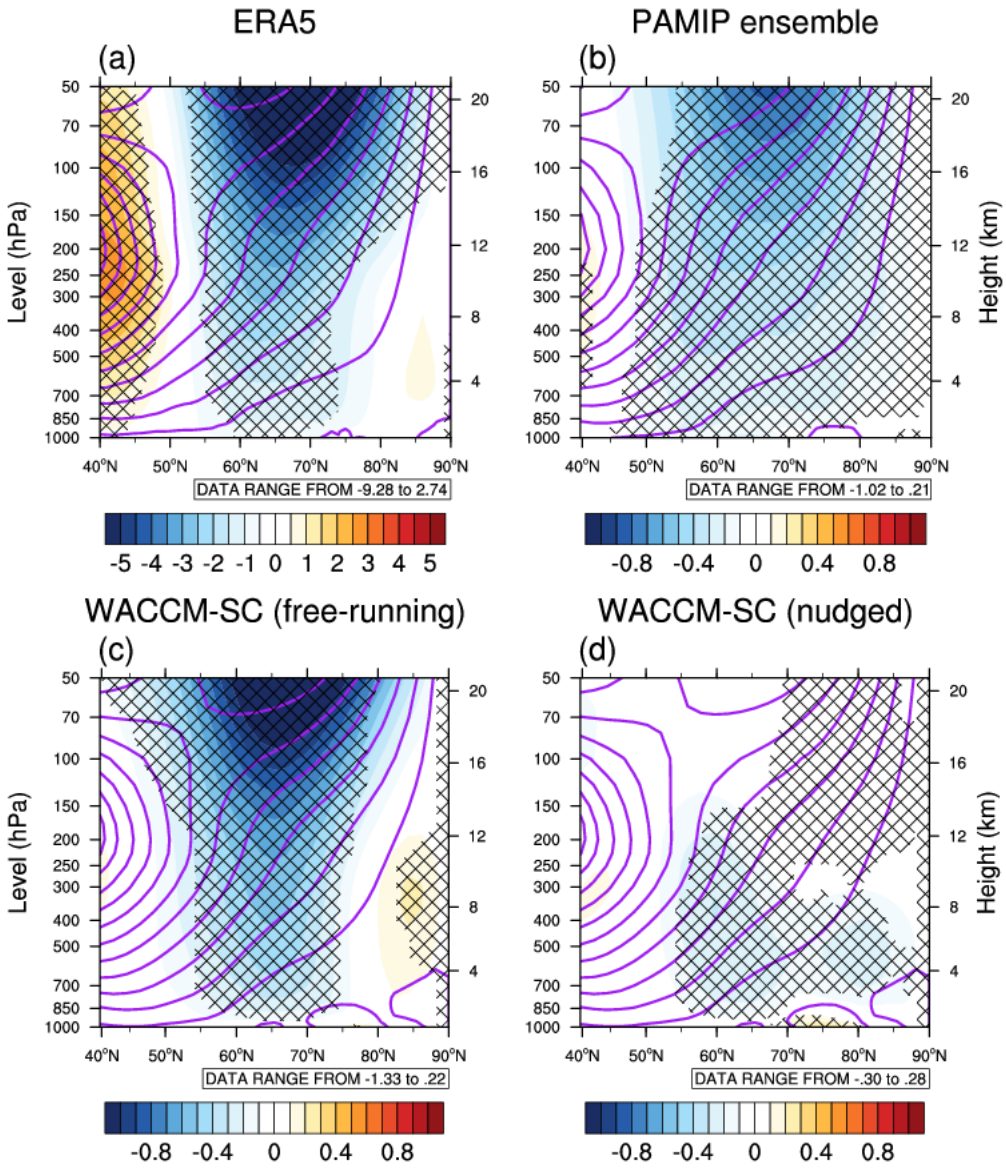

Supplementary Figure 4. Zonal-mean winter zonal wind anomalies induced by BKS sea-ice loss. (a) Zonal-mean winter zonal wind (shading; m s^{-1}) regressed against BKS sea ice, scaled by the composited SIC differences between BKS low- and high-SIC years, derived from the ERA5 reanalysis. Simulated zonal-mean winter zonal wind differences in the (b) PAMIP multi-model large ensemble results between pdSST-futBKSeasSIC and pdSST-pdSIC runs (scaled by the ratio between the observed BKS SIC index differences between low- and high-SIC years and the

PAMIP forcing), (c) free-running WACCM-SC simulations, and (d) nudged WACCM-SC simulations between LICE and HICE runs. Purple contours denote climatology of wintertime zonal-mean zonal wind derived from (a) ERA-5 1979-2020 data, (b) multi-model ensemble mean of pdSST-pdSIC runs from PAMIP and (c-d) WACCM CTRL run, with contour interval of 3 m s^{-1}. Hatched regions are statistically significant at the 90% confidence level according to bootstrap resampling statistical test.

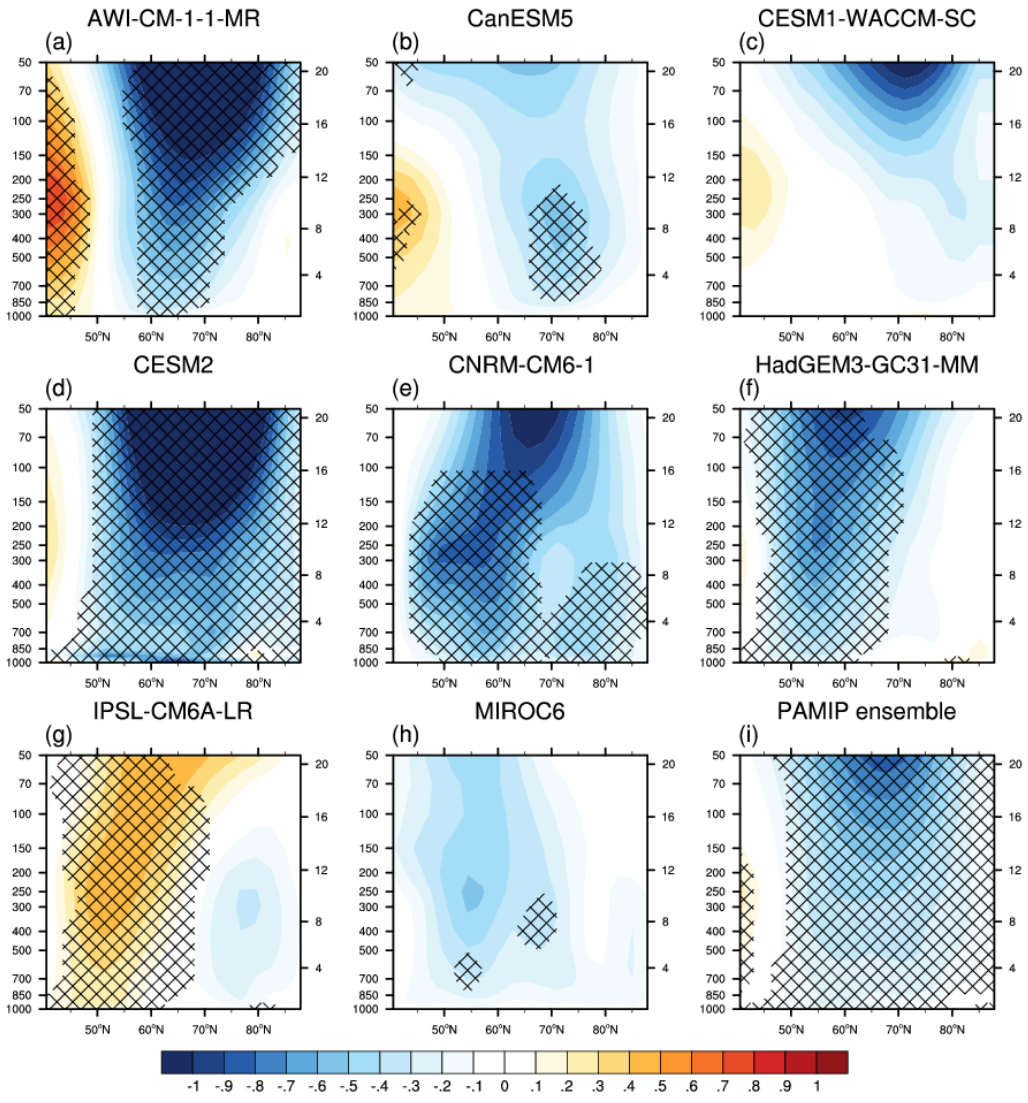

Supplementary Figure 5. Zonal-mean winter zonal wind anomalies induced by BKS sea-ice loss simulated by PAMIP models. Simulated wintertime zonal-mean winter zonal wind differences (m s^{-1}) between pdSST-futBKSeasSIC and pdSST-pdSIC runs from (a) AWI-CM-1-1-MR, (b) CanESM5, (c) CESM1-WACCM-SC, (d) CESM2, (e) CNRM-CM6-1, (f) HadGEM3-GC31-MM, (g) IPSL-CM6A-LR, (h) MIROC6 and (i) PAMIP multi-model ensemble mean. All the results are scaled by the ratio of the observed BKS SIC differences between low- and high-SIC years and PAMIP SIC forcing. Hatched regions are statistically significant at the 90% confidence level according to bootstrap resampling statistical test.

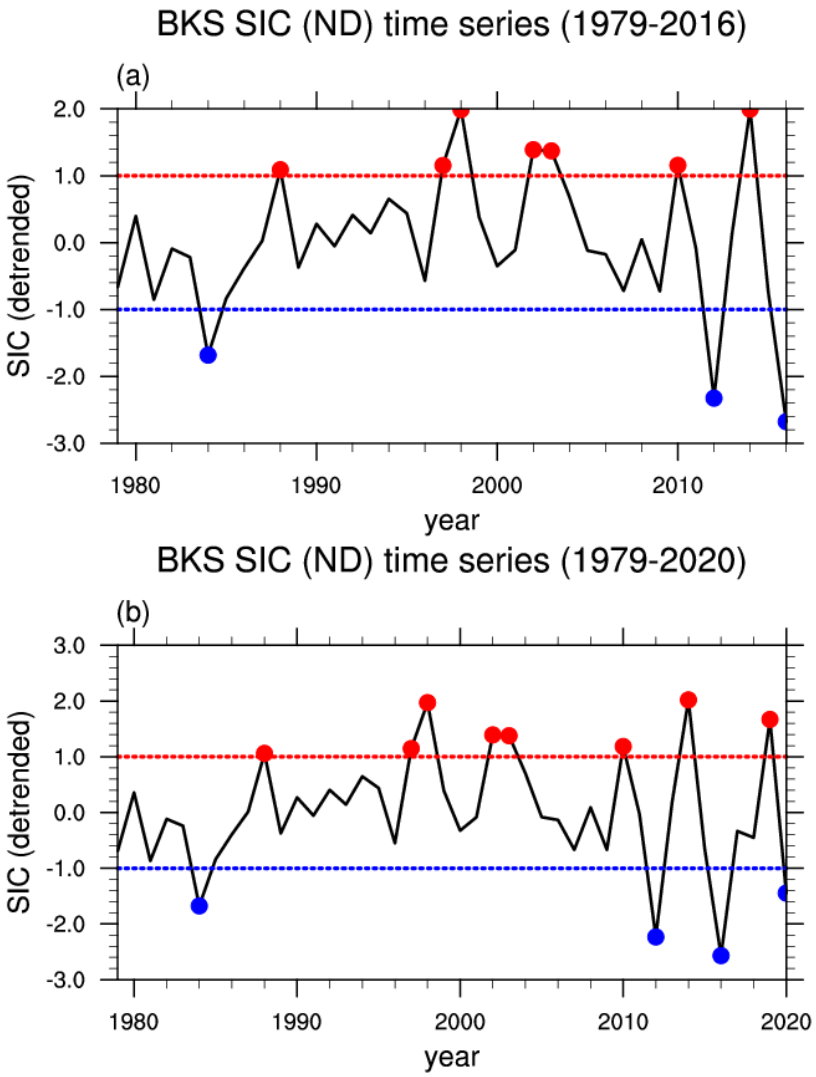

Supplementary Figure 6. Selection of BKS high- and low-SIC years. Time series of de-trended standardized (a) 1979-2016 and (b) 1979-2020 BKS SIC averaged in November and December (unit: 1), derived from HadISST1 dataset. Dashed blue/red line indicates the lower/upper threshold for the BKS low- and high-SIC years (1 time standard deviation) and the blue/red dots denote the selected BKS low- and high-SIC years using this criterion.

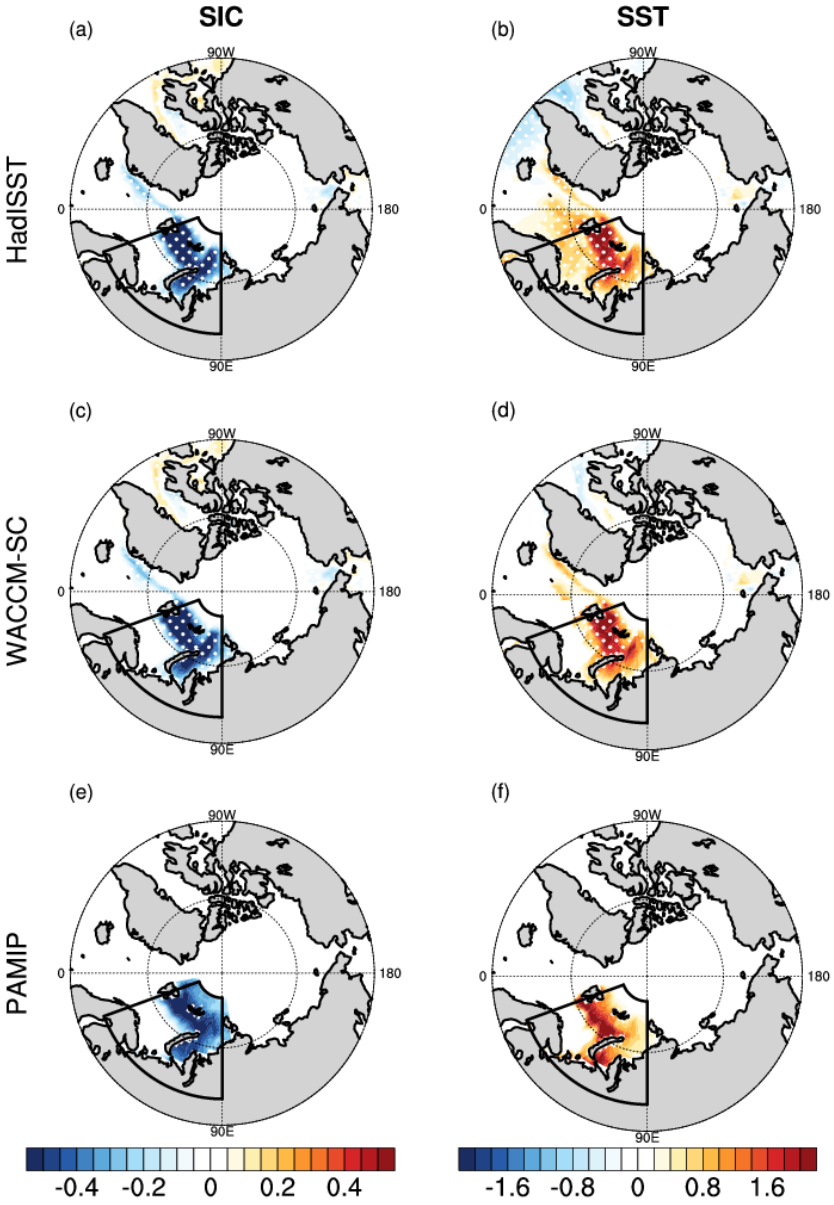

Supplementary Figure 7. SIC and SST differences between BKS low- and high-SIC years. Differences in (a) SIC (unit: %) and (b) SST (unit: °C) in early winter (November and December) between BKS low- and high-SIC years during 1979-2016, derived from HadISST1 data. (c, d) and (e, f) same as (a, b), but for prescribed boundary conditions of the WACCM-SC simulations and PAMIP experiments, respectively. The BKS region is outlined by the black box Hatched regions are statistically significant at the 90% confidence level according to bootstrap

resampling statistical test.

Supplementary Tables

Supplementary Table 1. List of the PAMIP models used. Table shows a list of the PAMIP models used in this study and their basic information.

Model name	Ensemble member	Horizontal grid (lon×lat)	Vertical levels	Model top (hPa)
AWI-CM-1-1-MR	100	384×192	95	0.01
CanESM5	100	128×64	49	1
CESM1-WACCM-SC	100	144×96	66	5.9e-06
CESM2	200	288×192	32	2.25
CNRM-CM6-1	100	256×128	91	~0.01
HadGEM3-GC31-MM	300	432×324	85	~0.01
IPSL-CM6A-LR	200	362×332	75	0.01
MIROC6	100	256×128	81	0.004